

Supplement of Atmos. Chem. Phys., 19, 14477–14492, 2019  
<https://doi.org/10.5194/acp-19-14477-2019-supplement>  
© Author(s) 2019. This work is distributed under  
the Creative Commons Attribution 4.0 License.



*Supplement of*

## **Quantifying the impact of synoptic circulation patterns on ozone variability in northern China from April to October 2013–2017**

**Jingda Liu et al.**

*Correspondence to:* Lili Wang (wll@mail.iap.ac.cn)

The copyright of individual parts of the supplement might differ from the CC BY 4.0 License.

1   **Text S1 Lamb-Jenkinson circulation typing approach**

2   In synoptic climatology, along with subjective or manual approaches, objective or automated  
3   approaches are important and widely used synoptic weather typing procedures to identify recurring  
4   map patterns or variable groups that typify significant modes of circulation and to classify each case  
5   into one of these modes (Yarnal, 1993; Huth et al., 2008). . There are many objective methods, such as  
6   correlation-based map-pattern technique, sums-of-squares method, rotated principal component  
7   analysis, hierarchical clustering (average linkage or Ward's clustering), and K-means clustering. As  
8   suggested by Huth (1996)and Yarnal (1993), , all the methods proved to be capable of yielding  
9   meaningful classifications and none of them can be thought of as the best in all aspects. Which method  
10   to use will depend mainly on the aim of the classification. Notably, the final number of synoptic types  
11   using these algorithms is associated with a given period and region, statistical algorithms, prior  
12   knowledge of the synoptic climatology of the region, and experimentation with various statistical  
13   procedures; finally, a subjective decision as to how many clusters are appropriate for the study period is  
14   made by the investigator. Thus, the results of a synoptic-type analysis are quite subjective.

15   The noted British climatologist Lamb developed a synoptic-scale, daily weather-map classification  
16   for use over the British Isles, and seven basic types were identified manually (Lamb, 1972). Based on  
17   Lamb's study, Jenkinson (1977) improved the subjective approach to an objective approach, called the  
18   Lamb-Jenkinson method (Jones et al., 1993; Trigo and DaCamara, 2000). According to the sea level  
19   pressure (SLP) of these 16 grids, a set of indices related to the direction and vorticity of geostrophic  
20   flow are calculated to determine the weather type. The indices used are the following: southerly flow  
21   component of the geostrophic surface wind (SF), westerly flow component of the geostrophic surface  
22   wind (WF), resultant flow (FF), southerly shear vorticity (ZS), westerly shear vorticity (ZW) and total  
23   shear vorticity (Z). These indices were computed using SLP values obtained for the retained number of  
24   grid points, and are both for the flow units as for the geostrophic vorticity expressed in hPa. As shown  
25   in 1a, the research area is placed in the central position, which refers to the area of connecting with P4,  
26   P8, P12, P13, P9 and P5. The SLP of 16 grids can be used to characterize the distance of between the  
27   study region and high-/low- pressure system, which result in the method is available to classify the  
28   weather pattern for each day and successfully applied in many areas (Lamb, 1972; Jenkinson, 1977;  
29   Trigo and DaCamara, 2000; Demuzere et al., 2009; Santurtún et al., 2015; Pope et al., 2016; Liao et al.,  
30   2017). The following presents the calculation methods for each index:

31    $SF=1.035\times[0.25\times(P5+2\times P9+P13)-0.25\times(P4+2\times P8+P12)]$

32    $WF=[0.5\times(P12+P13)-0.5\times(P4+P5)]$

33    $ZS=0.85\times[0.25(P6+2\times P10+P14)-0.25\times(P5+2\times P9+P13)-0.25\times(P4+2\times P8+P12)+0.25\times(P3+2\times P7+P11)]$

34    $ZW=1.12\times[0.5\times(P15+P16)-0.5\times(P8+P9)]-0.91\times[0.5\times(P8+P9)-0.5\times(P1+P2)]$

35    $F=(SF^2+WF^2)^{1/2}$

36    $Z=ZS+ZW$

37   P represents the SLP at the grid point. The positions of 16 grid points are shown in Fig. 1a; for example,  
38   P1 is the SLP at the 1st grid point.

39   The weather types are defined by comparing values of FF and Z:

40   (1) Direction of flow (in degrees) is given by  $\tan^{-1}(WF/SF)$ ,  $180^\circ$  being added if WF is positive. The  
41   appropriate wind direction is computed using an eight-point compass, allowing  $45^\circ$  per sector.

- 42 (2) If  $|Z| < FF$ , flow is essentially straight and considered to be of a pure directional type (eight  
 43 different possibilities according to the compass directions).  
 44 (3) If  $|Z| > 2FF$ , the pattern is considered to be of a pure cyclonic type if  $Z > 0$  or of a pure anticyclonic  
 45 type if  $Z < 0$ .  
 46 (4) If  $FF < |Z| < 2FF$ , flow is considered to be of a hybrid type and is therefore characterized by both  
 47 direction and circulation (16 different types).

48 Thus, compared with other objective synoptic classification approaches, the advantage of  
 49 Lamb-Jenkinson method is that the number of synoptic types and the weather type that is present each  
 50 day in the specific region is robust and fixed. In addition, the method clearly gives the typical pressure  
 51 fields (anticyclone, cyclone, directional types and hybrid types), which can well reflect the wind fields  
 52 over the study region. Particularly, directional types can represent the prevailing wind direction in this  
 53 area under the control of the specific weather pattern. Many studies have shown that the high/low  
 54 concentrations of ozone are always associated with the southerly/northerly winds in North China (Han  
 55 et al., 2019; Li et al., 2019). Consequently, the Lamb-Jenkinson weather type scheme is a better  
 56 method for exploring the O<sub>3</sub> pollution in North China.

## 57 **Text S2 Segmented synoptic-regression approach**

58 In an attempt to objectively define and weight the meteorological variables, Eder et al. (1994) indicated  
 59 that most influence the O<sub>3</sub> concentrations within each weather type, and they developed stepwise linear  
 60 regression models of the following form:

61  $O_3 = \beta_0 + \sum_{i=1}^n \beta_i x_i$  (1)

62 where O<sub>3</sub> represents the predicted MDA8 O<sub>3</sub> for each weather category,  $\beta_0$  is a constant,  $\beta_i$  represents  
 63 the coefficients (determined by the least squares method) of the independent meteorological variables  
 64  $x_i$ , and n is the number of independent meteorological variables in the equation. A stepwise regression  
 65 procedure was utilized because it sequentially identifies the ‘best subset’ of the independent  
 66 meteorological variables.

67 This paper used multiple linear regression with a stepwise method for variable selection to reconstruct  
 68 the time series for O<sub>3</sub> with F probability <0.05 to enter and F probability <0.10 to exit. After excluding  
 69 the missing data and disordering the time sequences, 80% of these days were used to build the potential  
 70 forecast equations and the remaining 20% were used to validate the accuracy of the equations.

## 71 **Tables**

72 **Table S1. Locations, period of available data, average MDA8 O<sub>3</sub> concentrations, and exceedance ratios of 58**  
 73 **cities. Abb, Lon, Lat and Alt are short for abbreviation, longitude, latitude and altitude, respectively.**

Province	City name	Abb	Lon	Lat	Alt	Period	O <sub>3</sub> ( $\mu\text{g m}^{-3}$ )	Exceedance Ratio (%)
Hebei	Chengde	CD	117.91	40.95	379.20	2013-2017	118	18.93
Hebei	Zhangjiakou	ZJK	114.87	40.81	860.20	2013-2017	114	15.84
Shanxi	Datong	DT	113.31	40.10	1051.17	2015-2017	112	9.38
Beijing	Beijing	BJ	116.38	40.04	58.25	2013-2017	127	29.43
Hebei	Qinhuangdao	QHD	119.60	39.93	2.80	2013-2017	102	9.56
Hebei	Tangshan	TS	118.18	39.63	6.83	2013-2017	124	25.12

Hebei	Langfang	LF	116.71	39.54	19.50	2013-2017	120	22.87
Shanxi	Shuozhou	SZ	112.43	39.34	1094.60	2015-2017	133	23.13
Tianjin	Tianjin	TJ	117.35	39.09	6.27	2013-2017	113	17.24
Hebei	Baoding	BD	115.47	38.87	15.00	2013-2017	125	25.68
Shanxi	Xinzhou	XZ	112.72	38.45	778.00	2015-2017	110	13.13
Hebei	Cangzhou	CZ	116.86	38.30	14.33	2013-2017	127	25.59
Hebei	Shijiazhuang	SJZ	114.48	38.03	153.75	2013-2017	116	21.18
Shanxi	Yangquan	YQ	113.56	37.86	767.83	2015-2017	119	20.63
Shanxi	Taiyuan	TY	112.52	37.86	800.89	2013-2017	116	18.67
Hebei	Hengshui	HS	115.68	37.74	23.00	2015-2017	138	34.86
Shanxi	Jinzhong	JZ	112.73	37.70	796.00	2015-2017	110	16.25
Shanxi	Lvliang	LL	111.13	37.51	943.00	2015-2017	88	3.75
Shandong	Yantai	YT	121.37	37.50	9.17	2015-2017	118	12.50
Shandong	Weihai	WH	122.09	37.49	26.00	2015-2017	115	9.53
Shandong	Dezhou	DZ	116.30	37.46	22.67	2015-2017	146	40.78
Shandong	Dongying	DY	118.64	37.43	3.25	2015-2017	146	35.94
Shandong	Binzhou	BZ	118.00	37.38	16.67	2015-2017	116	17.19
Hebei	Xingtai	XT	114.49	37.06	71.75	2013-2017	115	19.96
Shandong	Zibo	ZB	118.01	36.73	81.67	2015-2017	139	32.03
Shandong	Weifang	WF	119.14	36.71	53.80	2015-2017	142	34.38
Shandong	Jinan	JN	116.98	36.65	55.25	2015-2017	130	45.31
Hebei	Handan	HD	114.51	36.60	64.50	2013-2017	116	31.25
Shandong	Liaocheng	LC	115.99	36.45	44.67	2015-2017	133	29.06
Shandong	Laiwu	LW	117.69	36.21	207.67	2015-2017	123	21.56
Shandong	Tai'an	TA	117.11	36.19	170.00	2015-2017	126	22.81
Shanxi	Changzhi	CZH	113.11	36.19	924.40	2015-2017	141	36.72
Shandong	Qingdao	QD	120.39	36.15	23.78	2015-2017	105	12.66
Henan	Anyang	AY	114.37	36.09	84.20	2015-2017	119	22.03
Shanxi	Linfen	LFE	111.51	36.08	466.33	2015-2017	115	19.84
Henan	Hebi	HB	114.25	35.79	115.67	2015-2017	123	19.38
Henan	Puyang	PY	115.04	35.77	56.00	2015-2017	124	22.19
Shanxi	Jincheng	JC	112.85	35.50	743.17	2015-2017	103	15.94
Shandong	Jining	JN	116.59	35.42	34.00	2015-2017	135	31.09
Shandong	Rizhao	RZ	119.51	35.41	31.00	2015-2017	122	16.09
Henan	Xinxiang	XX	113.88	35.29	75.50	2015-2017	125	27.81
Shandong	Heze	HZ	115.45	35.25	47.00	2015-2017	131	25.00
Henan	Jiaozuo	JZ	113.23	35.22	93.00	2015-2017	122	23.91
Shanxi	Yuncheng	YC	111.02	35.05	380.20	2015-2017	117	19.06
Shandong	Linyi	LY	118.33	35.05	69.50	2015-2017	135	29.69
Shandong	Zaozhuang	ZZH	117.52	34.82	71.40	2015-2017	133	28.13
Henan	Kaifeng	KF	114.34	34.79	79.25	2015-2017	114	15.47
Henan	Sanmenxia	SMX	111.17	34.79	353.25	2015-2017	121	19.06
Henan	Zhengzhou	ZZ	113.65	34.78	111.44	2013-2017	101	17.34
Henan	Luoyang	LY	112.42	34.66	133.29	2015-2017	127	27.66

Henan	Shangqiu	SQ	115.66	34.42	33.25	2015-2017	124	18.44
Henan	Xuchang	XC	113.81	34.01	71.00	2015-2017	124	20.00
Henan	Pingdingshan	PDS	113.28	33.73	75.75	2015-2017	129	25.78
Henan	Zhoukou	ZK	114.66	33.61	45.75	2015-2017	116	13.28
Henan	Luohe	LH	114.03	33.57	65.75	2015-2017	127	22.81
Henan	Nanyang	NY	112.53	32.99	124.00	2015-2017	128	22.97
Henan	Zhumadian	ZMD	114.01	32.99	78.00	2015-2017	124	21.09
Henan	Xinyang	XY	114.06	32.12	89.50	2015-2017	110	10.31

74 **Table S2 Days of occurrence and the proportion of the most-polluted synoptic categories (LP and C) in May**  
75 **and the second half of May in each weather category in different years.**

	Year	N-E-S directions	S-W-N directions	LP	C	A	Proportion (%)
May	2013	5	14	4	4	4	25.8
	2014	7	16	3	4	1	22.6
	2015	7	10	4	4	6	25.8
	2016	8	12	2	2	7	12.9
	2017	5	13	3	8	2	35.5
	mean	6.4	13	3.2	4.4	4	24.5
The second half of May	2013	2	8	2	2	2	25.0
	2014	1	11	2	2	0	25.0
	2015	3	7	3	0	3	18.8
	2016	5	6	2	0	3	12.5
	2017	2	5	1	7	1	50.0
	mean	2.6	7.4	2	3.7	2.25	35.6

76

77      **Table S3 Equations of the multiple stepwise regressions for each weather type in 14 cities, where O<sub>3</sub> indicates  
78      MDA8 O<sub>3</sub>.**

Categories	Cities	Regression equation
N-E-S	CD	O <sub>3</sub> =4.77Tmax+9.97V+1.77ws-0.78RH_lag-1.16Tmax_lag+6.77V_lag+62.81
	ZJK	O <sub>3</sub> =2.1Tmax-5.26U-0.75RH_lag+0.79rain_lag+4.7V_lag+94.78
	BJ	O <sub>3</sub> =6.71Tmax+15.39V+12.22ws-0.66RH_lag-1.69Tmax_lag-9.49
	QHD	O <sub>3</sub> =2.2Tmax+11.25V+4.63
	TS	O <sub>3</sub> =-0.76RH+4.93Tmax+4.65U+17.05V+34.84
	LF	O <sub>3</sub> =-0.48RH+5.2Tmax+1.66V+1.87
	TJ	O <sub>3</sub> =4.69Tmax+3.96V-0.4RH_lag+5.53
	BD	O <sub>3</sub> =4.76Tmax+7.53V-0.49RH_lag-8.15U_lag+7.73V_lag+24.84
	CZ	O <sub>3</sub> =-0.57RH+4.73Tmax+8.69V-0.6wd_lag+41.47
	SJZ	O <sub>3</sub> =4.9Tmax-6U-0.54RH_lag+28.42
S-W-N	TY	O <sub>3</sub> =-0.41RH+2.53Tmax-0.92pre-3.62U+973.36
	XT	O <sub>3</sub> =6.22Tmax-5.14U-0.81RH_lag-1.82Tmax_lag+45.59
	HD	O <sub>3</sub> =-0.48RH+4.91Tmax+8.48
	ZZ	O <sub>3</sub> =3.47Tmax+1.89Tmax_lag+0.88rain_lag-55.75
	CD	O <sub>3</sub> =5.31Tmax-0.64RH_lag+8.89V_lag-1.53pre_lag+1579.54
	ZJK	O <sub>3</sub> =5.31Tmax-0.64RH_lag+8.89V_lag-1.53pre_lag+1579.54
	BJ	O <sub>3</sub> =7.86Tmax-7.72U+17.80V-79.97
	QHD	O <sub>3</sub> =-0.55RH+3.87Tmax+2.85V+48.73
	TS	O <sub>3</sub> =6.24Tmax+4.60U+10.64V-0.48RH_lag-0.06wd_lag+6.71
	LF	O <sub>3</sub> =6.7Tmax-1.66rain-0.46RH_lag+7.7V_lag-24.83
LP	TJ	O <sub>3</sub> =5.59Tmax+6.67V+4.67V_lag-43.81
	BD	O <sub>3</sub> =7.26Tmax-13.24ws-0.85RH_lag+18.28
	CZ	O <sub>3</sub> =5.16Tmax+4.86V-0.71RH_lag-0.7wd_lag+45.20
	SJZ	O <sub>3</sub> =6.25Tmax-11.2U-43.55
	TY	O <sub>3</sub> =-0.79RH+2.13Tmax-0.7wd-1.9pre-1.23U+212.60
	XT	O <sub>3</sub> =4.87Tmax-1.23rain+8.67ws-28.72
	HD	O <sub>3</sub> =4.61Tmax-1.54rain+5.15ws_lag-5.27
	ZZ	O <sub>3</sub> =4.58Tmax-2.64Tmax_lag+43.43
	CD	O <sub>3</sub> =4.39Tmax+15.62V-0.67RH_lag+56.36
	ZJK	O <sub>3</sub> =3.6Tmax+9.46V-0.8wd-0.33RH_lag+81.53
C	BJ	O <sub>3</sub> =7.14Tmax+18.59V-0.49RH_lag-32.17
	QHD	O <sub>3</sub> =3.33Tmax+22.46V+14.4ws+11.75
	TS	O <sub>3</sub> =-0.88RH+7.83Tmax+18.48V+11.00ws_lag+1.45pre_lag-1511.94
	LF	O <sub>3</sub> =8.72Tmax+1.36V+3.27pre-0.74RH_lag-7.47U_lag-3365.76
	TJ	O <sub>3</sub> =-0.5RH+6.2Tmax+6.45V-23.85
	BD	O <sub>3</sub> =-0.93RH+9.33Tmax+3.86pre-3951.69
	CZ	O <sub>3</sub> =-1.17RH+3.15Tmax-0.53rain-7.58ws_lag+142.22
	SJZ	O <sub>3</sub> =8.52Tmax-12.5U+2.65pre_lag-2785.79
	TY	O <sub>3</sub> =7.17Tmax-0.86RH_lag-14.71U_lag-1.68ws_lag-29.64
	XT	O <sub>3</sub> =7.7Tmax+2.22pre-2319.11
	HD	O <sub>3</sub> =5.88Tmax+2.67pre-2727.43
	ZZ	O <sub>3</sub> =3.33Tmax-22.58ws+44.13
	CD	O <sub>3</sub> =6.42Tmax+8.27V-0.97RH_lag+0.34rain_lag-11.62U_lag+1.75pre_lag-1746.67
C	ZJK	O <sub>3</sub> =4.16Tmax-8.24U+13.91
	BJ	O <sub>3</sub> =7.80Tmax+17.77V-0.49RH_lag-47.88

	QHD	O3=-0.99RH+3.2Tmax-2.33pre+246.27
	TS	O3=-1.15RH+8.10Tmax-2.13Tmax_lag+11.19V_lag+44.01
	LF	O3=8.47Tmax+9.52V-0.55RH_lag-75.33
	TJ	O3=-0.72RH+6.35Tmax+4.93V-13.34
	BD	O3=-0.78RH+6.35Tmax+7.89V+19.22
	CZ	O3=-1.59RH+4.39Tmax-5.45U+115.54
	SJZ	O3=-0.65RH+5.62Tmax-15.31U+8.26
	TY	O3=6.32Tmax-7.53U-69.28
	XT	O3=-0.51RH+6.26Tmax+0.12wd+6.37ws_lag-49.57
	HD	O3=-0.96RH+4.15Tmax+72.43
	ZZ	O3=6.29Tmax+2pre-289.95
A	CD	O3=-0.79RH+3.19Tmax+9.43V+8.73ws-1.73pre+5.83V_lag+1835.32
	ZJK	O3=-0.35RH+3.29Tmax+4.23V+6.17ws+4.26V_lag+4ws_lag+39.25
	BJ	O3=5.59Tmax-1.48pre-0.38RH_lag+1507.66
	QHD	O3=3.5Tmax+13.9V+12.17V_lag+7.48ws_lag+14.79
	TS	O3=5.83Tmax-0.66RH_lag+7.17V_lag+16.91
	LF	O3=6.45Tmax-44.57
	TJ	O3=6.47Tmax+6.99ws-0.43729RH_lag+3.58V_lag+1.37pre_lag-1433.13
	BD	O3=6.69Tmax-0.48RH_lag-13.34
	CZ	O3=7.64Tmax-0.63RH_lag-3.399Tmax_lag+7.11V_lag+51.58
	SJZ	O3=-0.43RH+6.19Tmax-16.88
	TY	O3=4.98Tmax+6.74ws_lag-38.97
	XT	O3=-0.39RH+5.77Tmax+3.228ws_lag-16.28
	HD	O3=-0.56RH+6.1Tmax-8.64
	ZZ	O3=4.57Tmax-0.6wd-1.394pre_lag+1399.78

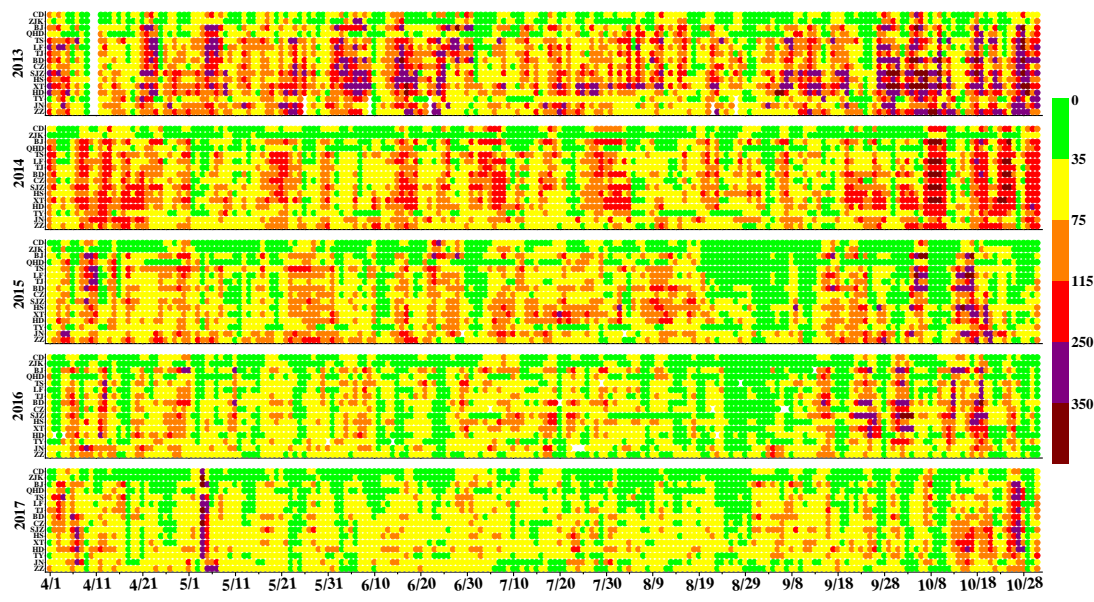
79 **Table S4. Three statistical measures ( $R^2$ , rmse, and CV) for the building and validation datasets for 5 weather  
80 categories and composite model for all 14 cities. Com: composite model (integration of each category's  
81 modeling results).  $R^2$  (%): variance in the individual model's coefficients of determination; rmse ( $\mu\text{g m}^{-3}$ ):  
82 root mean square error; and CV (%): coefficient of variation defined as rmse/mean MDA8 O<sub>3</sub>.**

Cities	Parameter	Building						Validation					
		com	HP	UP	LP	C	A	com	HP	UP	LP	C	A
CD	$R^2$	0.64	0.56	0.60	0.51	0.61	0.67	0.58	0.54	0.73	0.45	0.60	0.51
	RMSE	29.04	27.77	33.18	33.04	24.70	28.24	32.20	28.19	35.88	33.85	31.45	31.40
	CV	0.24	0.28	0.25	0.24	0.19	0.28	0.28	0.29	0.27	0.28	0.25	0.32
ZJK	$R^2$	0.53	0.36	0.56	0.45	0.31	0.62	0.61	0.47	0.83	0.34	0.89	0.68
	RMSE	29.48	28.25	32.38	31.54	32.34	24.47	34.01	26.78	40.77	44.94	28.03	28.70
	CV	0.26	0.29	0.26	0.25	0.26	0.24	0.30	0.30	0.31	0.39	0.22	0.29
BJ	$R^2$	0.64	0.57	0.65	0.54	0.59	0.64	0.69	0.67	0.73	0.67	0.47	0.65
	RMSE	36.28	35.07	37.62	42.32	36.94	33.28	37.44	36.49	33.42	42.00	39.74	38.71
	CV	0.29	0.35	0.27	0.29	0.25	0.31	0.29	0.35	0.23	0.28	0.28	0.36
QHD	$R^2$	0.36	0.24	0.33	0.33	0.24	0.43	0.40	0.37	0.54	0.36	0.23	0.46
	RMSE	34.25	31.64	34.88	39.31	40.03	28.51	36.29	29.71	37.94	44.32	38.58	33.75
	CV	0.34	0.36	0.32	0.33	0.35	0.32	0.36	0.38	0.31	0.42	0.36	0.36
TS	$R^2$	0.62	0.57	0.52	0.68	0.53	0.57	0.57	0.70	0.41	0.53	0.59	0.48
	RMSE	34.63	33.36	36.29	36.45	37.76	32.40	38.05	35.46	37.23	41.12	32.36	45.38
	CV	0.28	0.34	0.26	0.26	0.27	0.30	0.30	0.33	0.27	0.28	0.25	0.36

	$R^2$	0.63	0.61	0.60	0.60	0.60	0.65	0.63	0.89	0.55	0.39	0.56	0.68
LF	RMSE	31.79	29.57	33.03	36.76	34.22	28.90	34.26	27.80	32.41	40.90	41.39	32.30
	CV	0.27	0.28	0.26	0.28	0.26	0.27	0.29	0.31	0.26	0.27	0.28	0.32
TJ	$R^2$	0.59	0.55	0.51	0.53	0.48	0.67	0.71	0.63	0.81	0.70	0.62	0.85
	RMSE	30.65	28.28	33.59	33.58	34.08	25.31	28.62	26.11	29.69	24.56	34.28	26.76
BD	CV	0.27	0.30	0.28	0.26	0.26	0.26	0.26	0.29	0.25	0.18	0.28	0.27
	$R^2$	0.58	0.57	0.54	0.51	0.47	0.61	0.71	0.52	0.65	0.47	0.96	0.71
BD	RMSE	35.77	32.29	36.47	41.57	40.31	32.59	34.61	28.86	39.99	40.44	36.22	26.30
	CV	0.29	0.31	0.28	0.30	0.28	0.30	0.28	0.27	0.30	0.27	0.25	0.26
CZ	$R^2$	0.55	0.58	0.43	0.49	0.49	0.59	0.56	0.59	0.39	0.31	0.64	0.65
	RMSE	31.10	29.67	34.21	32.01	33.99	26.76	35.56	29.72	34.83	43.02	31.89	41.75
CZ	CV	0.25	0.27	0.25	0.23	0.24	0.24	0.28	0.26	0.25	0.30	0.22	0.43
	$R^2$	0.53	0.40	0.47	0.41	0.43	0.59	0.47	0.40	0.32	0.43	0.48	0.53
SJZ	RMSE	36.26	34.06	36.82	39.96	40.73	33.05	42.13	36.58	47.60	46.38	47.18	30.80
	CV	0.31	0.37	0.30	0.29	0.29	0.33	0.36	0.38	0.35	0.32	0.40	0.33
TY	$R^2$	0.46	0.41	0.37	0.38	0.26	0.49	0.50	0.36	0.29	0.61	0.39	0.52
	RMSE	34.54	26.49	36.56	40.26	42.37	30.96	34.73	26.77	39.70	37.03	38.29	31.26
TY	CV	0.39	0.39	0.41	0.38	0.37	0.42	0.41	0.38	0.42	0.39	0.37	0.46
	$R^2$	0.50	0.45	0.40	0.30	0.45	0.62	0.53	0.63	0.33	0.20	0.74	0.87
XT	RMSE	36.49	35.48	35.13	45.06	43.03	27.06	37.65	31.59	40.98	43.99	45.58	24.43
	CV	0.32	0.37	0.30	0.33	0.31	0.28	0.32	0.35	0.33	0.31	0.31	0.26
HD	$R^2$	0.45	0.43	0.35	0.18	0.34	0.54	0.50	0.54	0.40	0.17	0.57	0.53
	RMSE	36.41	33.66	35.83	45.31	41.09	30.25	34.40	31.37	35.42	39.19	38.32	28.81
ZZ	CV	0.31	0.35	0.28	0.34	0.31	0.31	0.31	0.33	0.28	0.29	0.33	0.32
	$R^2$	0.25	0.32	0.08	0.12	0.14	0.45	0.24	0.32	0.12	0.18	0.28	0.48
ZZ	RMSE	47.22	39.60	50.19	55.78	57.67	35.32	48.88	40.72	49.63	64.64	55.83	35.87
	CV	0.48	0.44	0.51	0.50	0.48	0.44	0.48	0.49	0.54	0.52	0.39	0.43

83 **Figures**

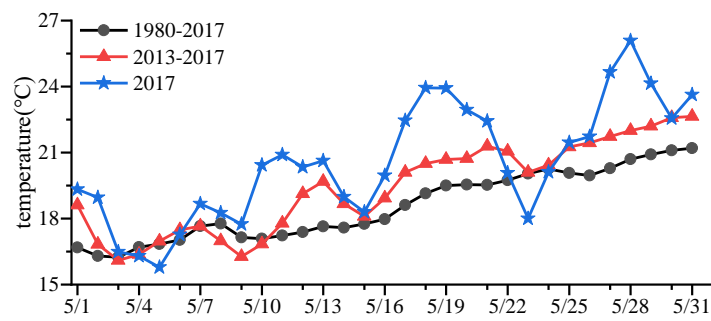
84



85

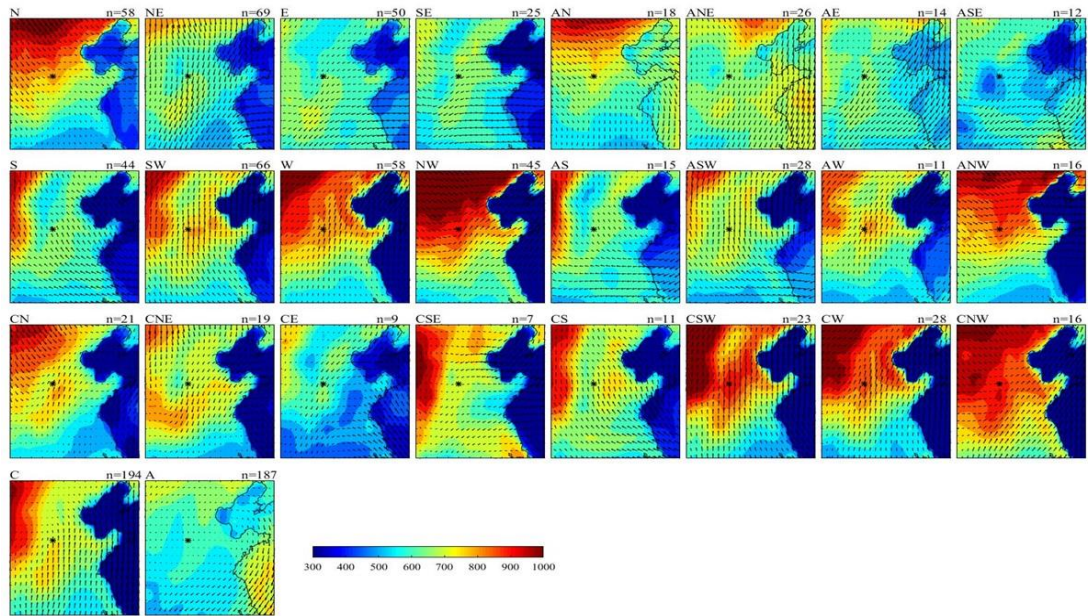
**Fig. S1.** Time series of daily averaged PM<sub>2.5</sub> concentrations in 14 cities (north to south) during April to October from 2013 to 2017. Six ranks are separated, representing different air-quality levels, including excellent (green spots), good (yellow), lightly polluted (orange), moderately polluted (red), heavily polluted days (purple) and severely polluted (maroon) with cut-off concentrations as 35, 75, 115, 150 and 250  $\mu\text{g m}^{-3}$ , respectively.

90



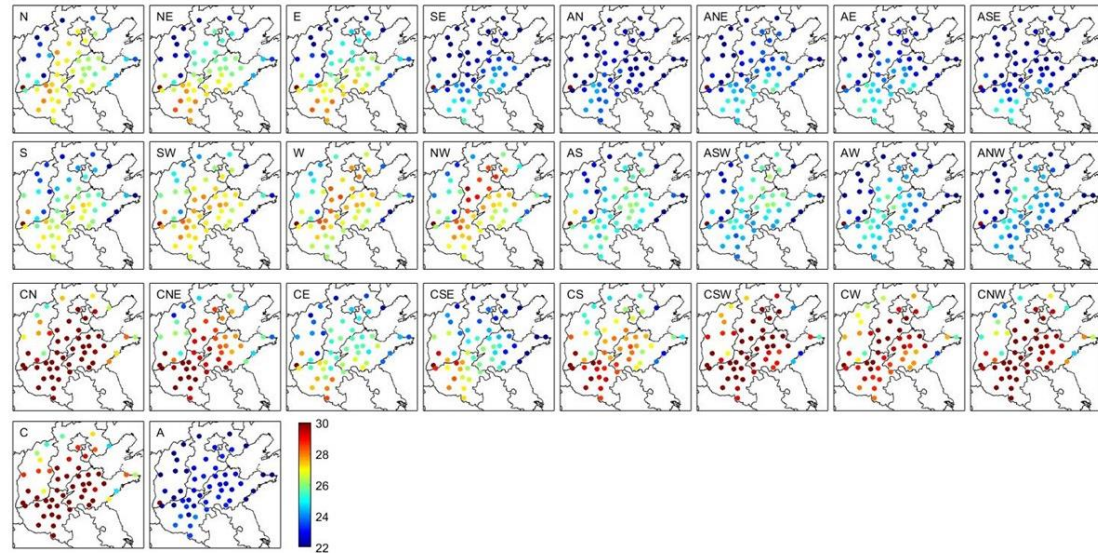
91

**Fig. S2.** Time series of the daily average temperature from 1980-2017, 2013-2017 and 2017.



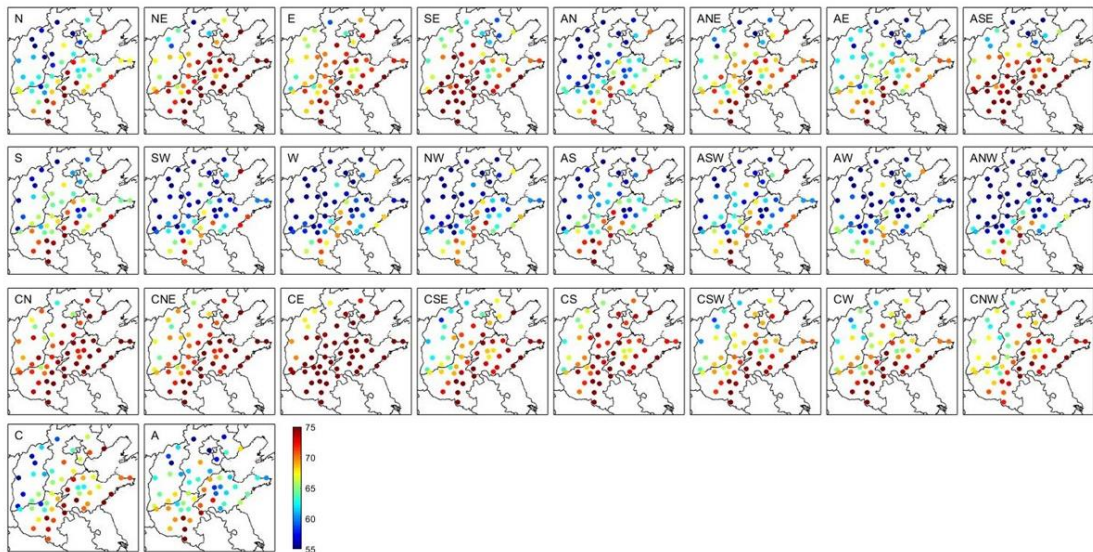
92

93 **Fig. S3. Wind field and boundary layer height (based on ERA-interim data) and occurrence days under**  
 94 **different weather conditions. The colour shading corresponds to the mean boundary layer height. The black**  
 95 **“\*” indicates the center of North China.**



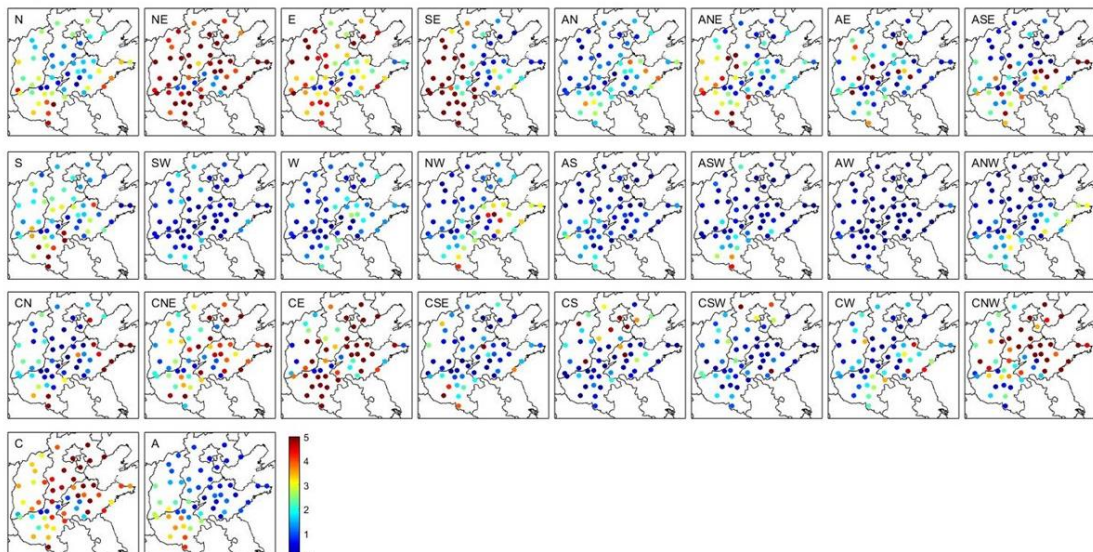
96

97 **Fig. S4. Spatial distributions of average temperature for the 26 weather types. The first, second, and third**  
 98 **rows correspond to the N-E-S direction, S-W-N direction, and LP, respectively; the fourth row from left to**  
 99 **right is C and A, respectively.**



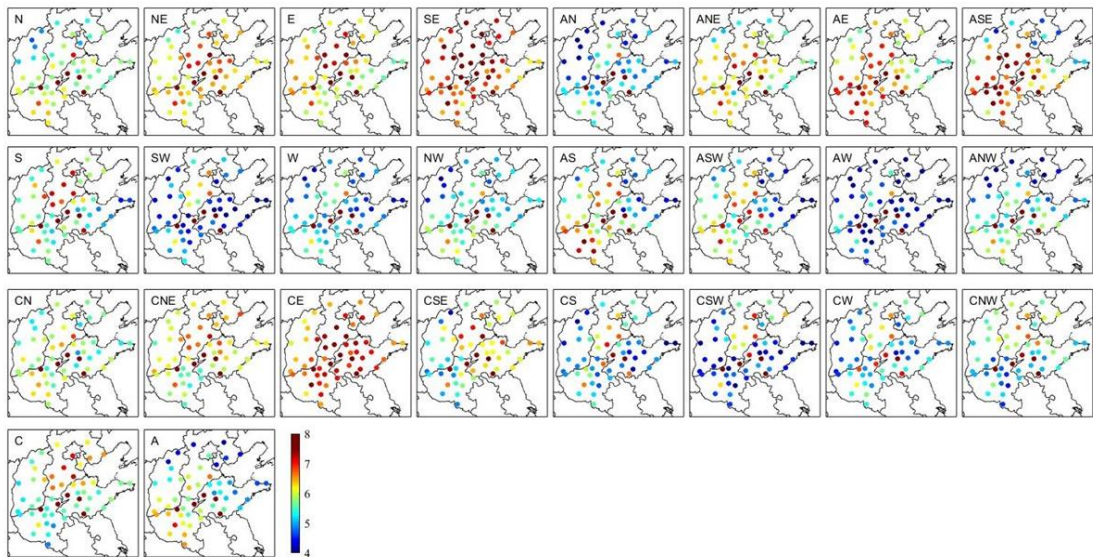
100

101 **Fig. S5.** Same as Fig. S4 but for RH (%).



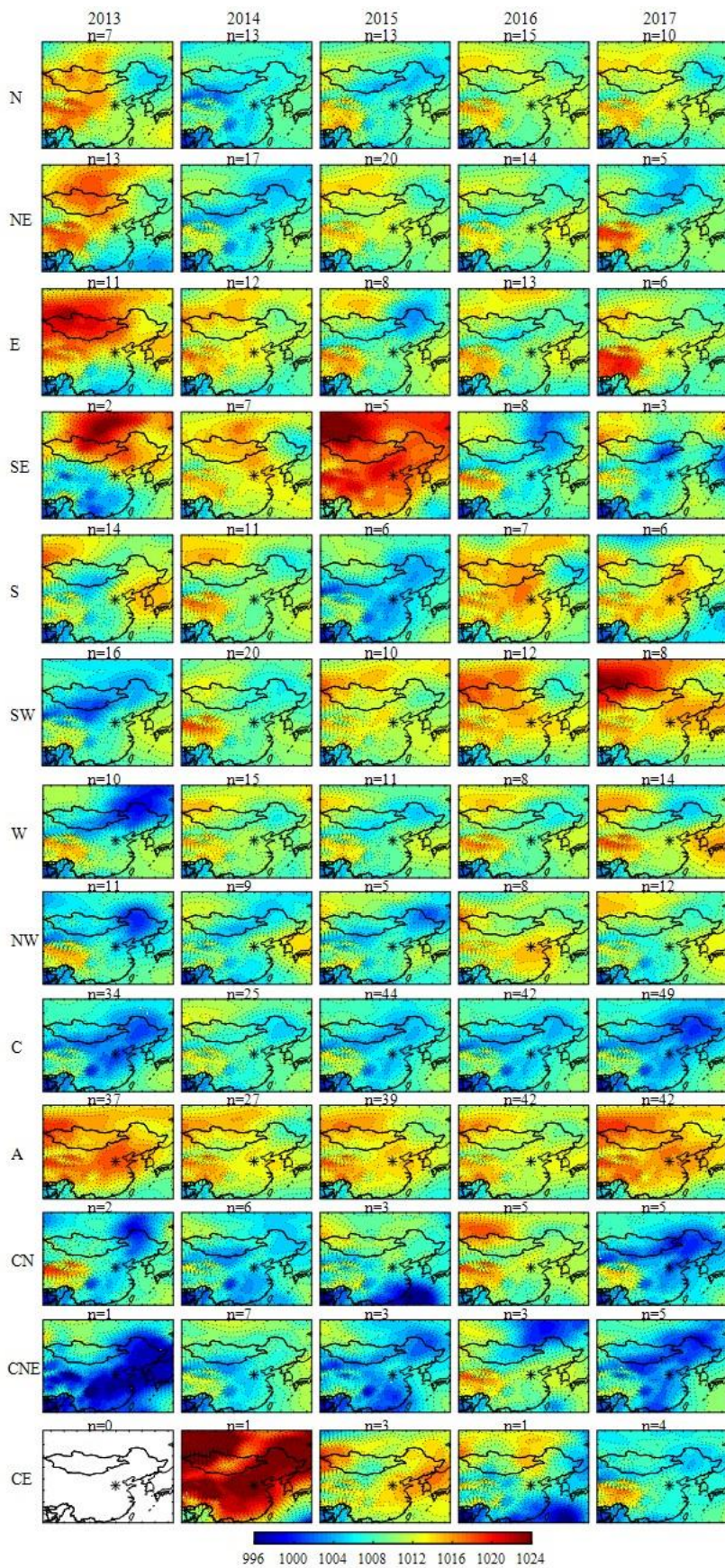
102

103 **Fig. S6.** Same as Fig. S4 but for rain (mm).



104

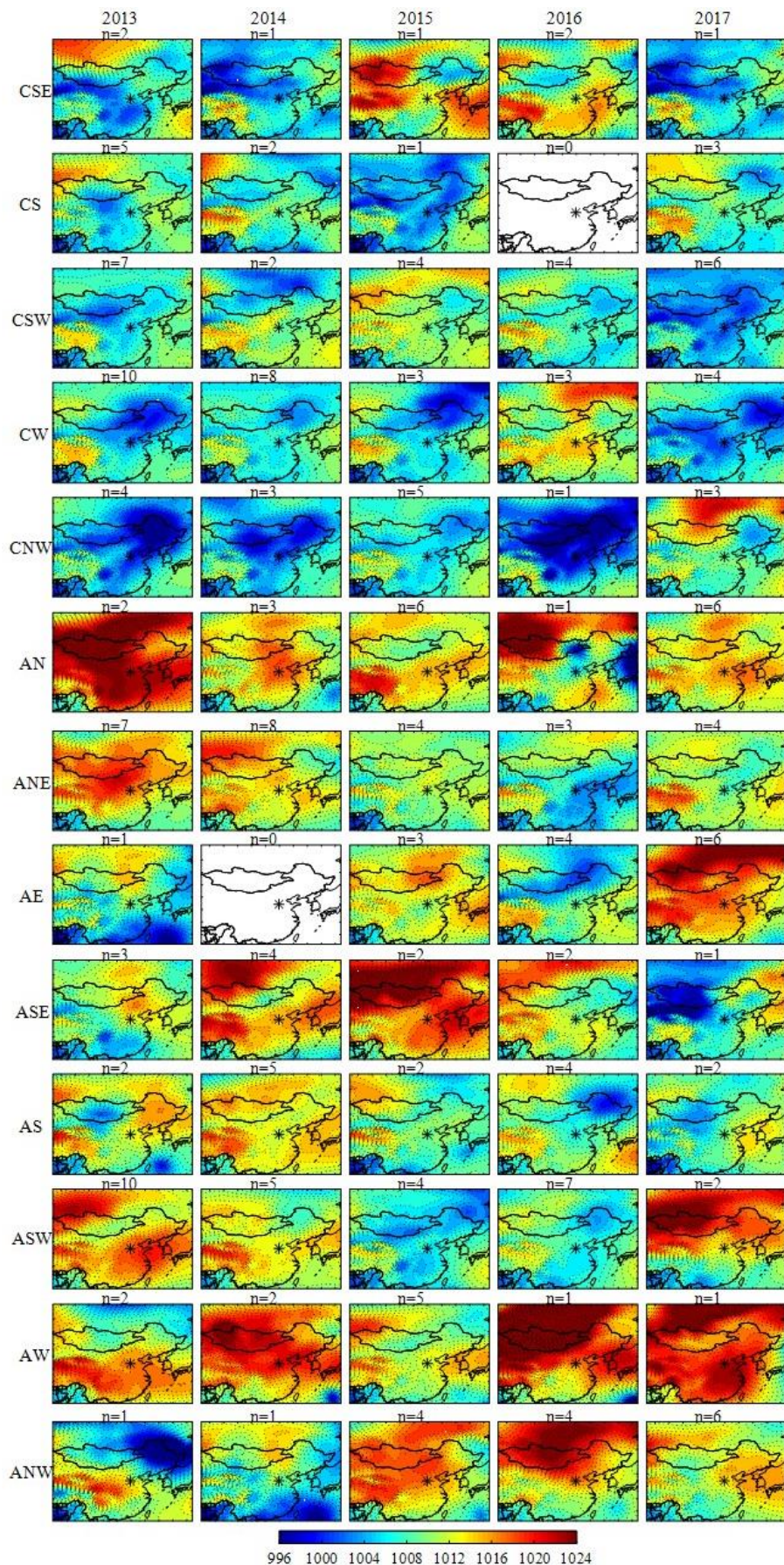
105 **Fig. S7. Same as Fig. S4 but for TCC.**



106

107

**Fig. S8. Pressure field characteristics and occurrence days (n) of weather type N to CE in 2013-2017.**

**Fig. S9. Pressure field characteristics and occurrence days (n) of weather type CSE to ANW in 2013-2017.**

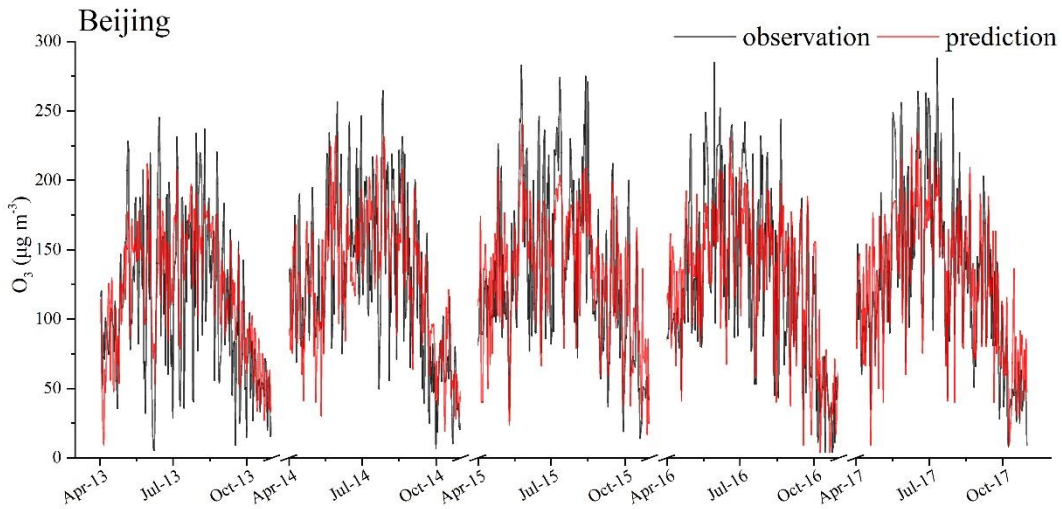


**Fig. S10. Comparison of the observed and predicted values in Beijing from April-October 2013-2017.**

### References

- Demuzere, M., Trigo, R. M., Vila-Guerau de Arellano, J., and van Lipzig, N. P. M.: The impact of weather and atmospheric circulation on O<sub>3</sub> and PM<sub>10</sub> levels at a rural mid-latitude site, *Atmos. Chem. Phys.*, 9, 2695-2714, <https://doi.org/10.5194/acp-9-2695-2009>, 2009.
- Eder, B. K., Davis, J. M., and Bloomfield, P.: An Automated Classification Scheme Designed to Better Elucidate the Dependence of Ozone on Meteorology, *J.appl.meteor*, 33, 1182-1199, 1994.
- Han, H., Liu, J., Shu, L., Wang, T., and Yuan, H.: Local and synoptic meteorological influences on daily variability of summertime surface ozone in eastern China, *Atmospheric Chemistry and Physics Discussions*, 1-51, [10.5194/acp-2019-494](https://doi.org/10.5194/acp-2019-494), 2019.
- Huth, R.: An intercomparison of computer-assisted circulation classification methods, *International Journal of Climatology: A Journal of the Royal Meteorological Society*, 16, 893-922, 1996.
- Huth, R., Beck, C., Philipp, A., Demuzere, M., Ustrnul, Z., Cahynová, M., Kyselý, J., and Tveito, O. E.: Classifications of atmospheric circulation patterns, *Annals of the New York Academy of Sciences*, 1146, 105-152, 2008.
- Jenkinson, A. F., Collison, F.P: An initial climatology of gales over the North Sea. , Synoptic Branch Memorandum No. 62. Met Office, Exeter., 1977.
- Jones, P. D., Hulme, M., and Briffa, K. R.: A comparison of Lamb circulation types with an objective classification scheme, *International Journal of Climatology*, 13, 655-663, 1993.
- Lamb, H. H.: British Isles weather types and a register of the daily sequence of circulation patterns, 1861–1971., *Geophysical Memoir.*, 116, p. 85., 1972.
- Li, K., Jacob, D. J., Liao, H., Shen, L., Zhang, Q., and Bates, K. H.: Anthropogenic drivers of 2013–2017 trends in summer surface ozone in China, *Proceedings of the National Academy of Sciences*, 116, 422-427, [10.1073/pnas.1812168116](https://doi.org/10.1073/pnas.1812168116), 2019.
- Liao, Z., Gao, M., Sun, J., and Fan, S.: The impact of synoptic circulation on air quality and pollution-related human health in the Yangtze River Delta region, *The Science of the total environment*, 607-608, 838-846, [10.1016/j.scitotenv.2017.07.031](https://doi.org/10.1016/j.scitotenv.2017.07.031), 2017.

- 139 Pope, R. J., Butt, E. W., Chipperfield, M. P., Doherty, R. M., Fenech, S., Schmidt, A., Arnold, S. R., and Savage,  
140 N. H.: The impact of synoptic weather on UK surface ozone and implications for premature mortality,  
141 Environmental Research Letters, 11, 124004, 10.1088/1748-9326/11/12/124004, 2016.
- 142 Santurtún, A., González-Hidalgo, J. C., Sanchez-Lorenzo, A., and Zarrabeitia, M. T.: Surface ozone concentration  
143 trends and its relationship with weather types in Spain (2001–2010), Atmospheric Environment, 101, 10-22, 2015.
- 144 Trigo, R. M., and DaCamara, C. C.: Circulation weather types and their influence on the precipitation regime in  
145 Portugal, International Journal of Climatology, 20, 1559-1581, 2000.
- 146 Yarnal, B.: Synoptic climatology in environmental analysis: a primer, Belhaven, 1993.
- 147